ANTICANCER RESEARCH *40*: 3209-3220 (2020)
doi:10.21873/anticanres.14302

Tannic Acid Inhibits Non-small Cell Lung Cancer (NSCLC) Stemness by Inducing G_0/G_1 Cell Cycle Arrest and Intrinsic Apoptosis

NIPIN SP[1*], DONG YOUNG KANG[1*], DOH HOON KIM[1*], JI-SEUNG YOO[2], EUN SEONG JO[1], ALEXIS RUGAMBA[1], KYOUNG-JIN JANG[1] and YOUNG MOK YANG[1]

[1]*Department of Pathology, School of Medicine, Institute of Biomedical Science and Technology, Konkuk University, Seoul, Republic of Korea;*
[2]*Department of Immunology, Hokkaido University Graduate School of Medicine, Sapporo, Japan*

Abstract. *Background/Aim: Non-small cell lung cancer (NSCLC) is one among the most common cancers worldwide. Recently, dietary phytochemicals have been reported as an attractive approach to improve the symptoms of NSCLC patients. Tannic acid is a natural polyphenol, which is known to have anticancer effects on in vitro models of breast, gingival and colon cancer. However, the molecular mechanisms associated with the actions of tannic acid on A549 human lung cancer cells have not been elucidated. Materials and Methods: In this study, we analyzed the effect of tannic acid on A549 cells and their underlying mechanisms using western blotting, flow cytometry, invasion assay and tumorsphere formation assay. Results: Tannic acid treatment suppressed the viability of A549 cells through cell cycle arrest and induction of the intrinsic pathways of apoptosis. In addition, the various malignant phenotypes of A549 cells including invasion, migration, and stemness were inhibited by tannic acid treatment. Conclusion: Tannic acid could be used as an effective inhibitor of lung cancer progression.*

Non-small cell lung cancer (NSCLC) accounts for about 80% of the lung cancer cases and is one of the most common carcinomas in the world (1). For NSCLC patients, chemotherapy, radiation therapy and surgical resection are used as treatment depending on the size of the tumor and the success of the treatment (2). Chemotherapy is particularly used in cases where surgery or radiotherapy is not recommended or generally used before or after radiotherapy and surgery (3). However, the success of chemotherapy remains low due to late diagnosis, drug resistance, recurrence, and serious side effects of platinum based drugs (4, 5). Therefore, there is need for continuous efforts to improve the therapeutic regimens and reduce side effects of chemotherapy.

Cancer chemoprevention with dietary phytochemicals is an attractive approach to prevent, cure or delay the progression of cancer (6, 7) as well as to contribute to the immune system regulation (8). Several phytochemicals that we routinely consume have been reported to inhibit carcinogenesis *via* various mechanisms (9-11) including the regulation of cell cycle, cell death, invasion, migration, stemness phenotype, and cellular signaling pathways.

Tannic acid (TA) is a natural polyphenol present in plants and is known to possess anti-cancer, anti-inflammatory and antioxidant properties (12, 13). Because tannic acid has many hydroxyl groups as functional groups, it can regulate the oncogenic signals by directly binding to the biological macromolecules (13). For instance, tannic acid is known to inhibit the viability of breast cancer cells by binding to the cell surface growth factor receptors including the epidermal growth factor receptor (EGFR), insulin-like growth factor receptor (IGFR), and estrogen receptors (12). Furthermore, in gingival cancer, tannic acid has been reported to down-regulate signal transducer and activator of transcription 3 (STAT3) signal and cell viability (14). A recent study has shown that tannic acid could induce programmed cell death in embryonic cancer stem cells by promoting TRAIL-mediated apoptosis (15). However, the effects and associated mechanisms of tannic acid on lung cancer cells have not been explored so far.

*These Authors contributed equally to this work.

Correspondence to: Kyoung-Jin Jang, Department of Pathology, School of Medicine, Institute of Biomedical Science and Technology, Konkuk University, Seoul, Republic of Korea. Tel: +82 220307839, e-mail: jangkj@konkuk.ac.kr; Young Mok Yang, Department of Pathology, School of Medicine, Institute of Biomedical Science and Technology, Konkuk University, Seoul, Republic of Korea. Tel: +82 220307812, e-mail: ymyang@kku.ac.kr

Key Words: Lung cancer, tannic acid, intrinsic apoptosis, G_0/G_1 cell cycle arrest.

The current study investigated the molecular signaling of the inhibitory effects of tannic acid on A549 cells, a typical NSCLC model. We evaluated the effects of tannic acid on cell death, cell cycle, and metastatic potential including invasion, migration, and sphere forming ability of A549 cells.

Materials and Methods

Reagents. Tannic acid (20 mM/l) dissolved in D.W was stored in the dark at 4˚C and diluted in RPMI-1640 medium (Gibco, Grand Island, NY, USA) immediately before use. Crystal violet, DAPI and propidium iodide (PI) were obtained from Sigma-Aldrich (Sigma-Aldrich, St. Louis, MO, USA). NE-PER cytoplasmic and nuclear extraction reagents were obtained from Thermo Fisher Scientific Inc (Thermo Fisher Scientific Inc, Rockford, IL, USA). Antibodies specific to cleaved PARP, cleaved caspase 9, BCL2, Bax, and cytochrome c were purchased from Cell Signaling Technology (Cell Signaling Technology, Danvers, MA, USA). The anti-mouse IgG HRP-conjugated secondary antibody, anti-rabbit IgG horseradish peroxidase (HRP) conjugated secondary antibody and tannic acid were supplied by Merck (Merck, Darmstadt, Germany). Antibodies against p27, cyclin D, cyclin E, CDK4, retinoblastoma (Rb), phospho-Rb, actin, NDRG-1, Actin, PE conjugated CD133 and GAPDH were purchased from Santa Cruz Biotechnology (Santa Cruz, CA, USA). 3,3'-dihexyloxacarbocyanine iodide (DiOC6) was obtained from Enzo (Enzo, Farmingdale, NY, USA). Z-VAD-FMK was supplied by R&D Systems, Inc. (R&D Systems, Minneapolis, MN, USA) and FITC-Annexin V apoptosis detection kit I and Matrigel invasion chambers was obtained from BD Biosciences (BD Biosciences, San Jose, CA, USA). Mitochondria isolation kit was supplied by Thermo scientific (Thermo Fisher Scientific Inc, Rockford, IL, USA).

Cell culture. A549 cells were obtained from the American Type Culture Collection (ATCC) (Manassas, MD, USA). Cells were maintained and sub-passaged in RPMI 1640 with 10% fetal bovine serum (FBS; Invitrogen, Carlsbad, CA, USA) and 1% antibiotic-antimycotic (ABAM; Invitrogen, Carlsbad, CA, USA). Cells were maintained in a humidified atmosphere with 5% CO_2 at 37˚C. Routinely, media were replaced every 2 days. At 75% confluence, cells were gently washed twice with PBS and harvested by centrifugation with 0.05% trypsin-ethylene diamine tetra acetic acid (trypsin-EDTA; Welgene, Gyeongsan-si, Republic of Korea).

Crystal violet assay. 1×10^4 cells per 100 μl medium/well A549 cells were seeded in 96-well culture plates. Then cells were incubated and treated at 75% confluence with different concentrations of tannic acid for 24 h. Cell viability was accessed by crystal violet assay (20). The absorbance was measured at 595 nm on an Ultra Multifunctional Microplate Reader (TECAN, Durham, NC, USA). All measurements were performed three times and the experiments were repeated at least three times.

DAPI staining and morphological analysis. Apoptotic condensed chromatin was examined by DAPI staining. A549 cells were seeded in 6-well plates at a density of 1.5×10^5 cells/well and treated with different concentrations of tannic acid for 24 h, after which the cells were washed twice with PBS. Then, 500 μl of 300 nM DAPI staining solution were added and the cells were washed two times with PBS. Stained cells were mounted with mounting solution on microscope slides and observed by fluorescence microscopy (Olympus, Tokyo, Japan).

Annexin V and PI staining. 1.5×10^5 A549 cells/ml were seeded into 6 cm culture dishes, treated with tannic acid for 24 h, harvested using trypsin-EDTA and washed twice with PBS. Apoptosis was assayed using the FITC-Annexin V apoptosis detection kit I according to the manufacturer's instructions. Data were analyzed using a Fluorescence-activated cell sorting (FACS) Calibur instrument and Cell Quest software (BD Biosciences, San Jose, CA, USA).

Cell cycle analysis. Cell cycle analysis was performed by flow cytometry with PI staining. A549 cells (1.5×10^5 cells/ml) were seeded into 6 cm culture dishes and treated with increasing concentrations of tannic acid for 24 h. Cells were harvested with trypsin-EDTA, then fixed with 75% ethanol. Next, the cells were washed two times with cold PBS and the supernatant was discarded after centrifugation. The pellet was re-suspended and stained with 50 μg/ml of PI and 100 μg/ml of RNase A for 20 min in the dark. DNA content was analyzed by flow cytometry using a FACS Calibur instrument and Cell Quest software (BD Biosciences).

Wound healing assay. 1×10^5 A549 cells/well were cultured in 6-well plates and incubated for 24 h. After becoming a confluent monolayer, the cells were scratched with a 10 μl pipette tip and washed with PBS to remove cell debris. Cells were treated with different concentrations of tannic acid for 24 h. Wound closure was photographed at 0 h and 24 h using a microscope. The relative area of wound closure was measured using Image J software (NIH Image, Bethesda, MD, USA).

Matrigel invasion assay. The trans-well invasion assay was conducted in invasion chambers (BD Biosciences, Andover, MA, USA). 5×104 A549 cells were added to the inserts. The media containing different concentrations of TA were added to the receiver plate and the inserts containing cells were placed on top of it. After a 24 h incubation in a humidified chamber at 37˚C, the invaded cells in the apical surface of the inserts were stained with crystal violet. The cells on the upper surface were removed using a cotton swab and the invaded cells were observed under a microscope.

Tumor sphere formation assay. Tumor sphere assay was performed by culturing A549 cells (5×10^3 cells/well) in DMEM/F12 media containing growth supplements including EGF, bFGF and B27 in low attachment 6 well plates. The treatment started at day 0 and incubation continued for 7 days. Photographs were taken at day 0, 4, 7 using a microscope. Total RNA was isolated from the spheres and analyzed using RT-PCR. Tumor sphere number was counted with microscope.

Analyses of CD133 expression. CD133 expression analysis was performed using PE-conjugated CD133 antibody and flow cytometry. A549 cells (1.5×10^5 cells/ml) were seeded into 60 mm culture dishes and treated with different concentrations of tannic acid for 24 h. Cells were harvested with trypsin-EDTA and were washed twice with cold PBS and centrifuged to discard the supernatant. The pellet was re-suspended and stained with PBS containing PE-conjugated CD133 antibody for 30 min in the dark. Then cells were analyzed by flow cytometry using a FACS Calibur instrument and Cell Quest software (BD Biosciences).

Table I. *RT-PCR primer sequences, annealing temperature and product sizes.*

Gene	Sequence (5' to 3')	Annealing Tm (°C)	Product size (bp)
SOX2	Forward: GTGGAAACTTTTGTCGGAGA Reverse: GGCAGCGTGTACTTATCCTT	56	150
OCT4	Forward: CACGTAGGTTCTTGAATCCC Reverse: CACATCGGCCTGTGTATATC	56	185
NANOG	Forward: AAAAGGAAGACAAGGTCCCA Reverse: CCTGTTTGTAGCTGAGGTTC	56	159
NDRG1	Forward: GAACCACAAAACCTGCTACA Reverse: GACTCCAGGAAGCATTTCAG	56	175
GAPDH	Forward: CAACTACATGGCTGAGAACG Reverse: GATGATGACCCTTTTGGCTC	56	190

RNA extraction and cDNA synthesis. Total RNA was extracted from A549 cells by TRIzol (Invitrogen, Karlsruhe, Germany). A total of 200 μl of chloroform were added and the mixture was incubated at 4˚C for 5 min, and then centrifuged at 4˚C for 15 min. The supernatant was removed, mixed with isopropanol, and incubated at 4˚C for 15 min to collect RNA pellets. Isopropanol was removed from the solution by centrifuging at 4˚C for 15 min. Then, it was washed with 75% ethanol and dissolved in RNase-Free Water. The RNA purity was measured by measuring the absorbance at 230 nm and 260 nm using a spectrophotometer (ND-100, Nanodrop Technologies Inc., Wilmington, DE, USA). To synthesize cDNA, 1 μg of RNA and 1 μl each of oligo-dT (Invitrogen, MA) and RNase-Free Water were added. The RNA was denatured at 80˚C for 3 min, and cDNA was synthesized using 4 μl of 5×RT (reverse transcription) buffer, 5 μl of 2 mM dNTPs, 0.5 μl of RNase inhibitor (Promega, Madison, WI, USA), and 1 μl of M-MLV (Moloney-murine leukemia virus) RT (Promega).

Reverse transcription polymerase chain reaction (RT-PCR). The primers for the amplification of the genes (Table I) were synthesized using PRIMER3 software. RT-PCR was performed by a C1000 Thermal Cycler (Bio Rad, Hercules, CA, USA). The composition of the reaction solution was as follows: 2 μl cDNA (50 ng/μl) was added to 16 μl master mix (Bio Rad) and 1 μl each of 5 pmol/μl forward and reverse primers. The conditions of the RT-PCR were, initial denaturation at 94˚C for 10 min followed by 35 cycles of denaturation at 94˚C for 30 s, annealing at 60˚C for 30 s, and extension at 72˚C for 30 s. *GAPDH* was used as reference gene.

Western blot analysis. Cells were treated with different concentrations of tannic acid for 24 h, harvested, washed with PBS, and centrifuged (1,890 × *g*, 5 min, 4˚C). The resulting cell pellets were re-suspended in lysis buffer containing 50 mM Tris (pH 7.4), 1.5 M sodium chloride, 1 mM EDTA, 1% NP-40, 0.25% sodium deoxycholate, 0.1% sodium dodecyl sulfate (SDS), and a protease inhibitor cocktail. The cell lysates were incubated on ice for 1 h and supernatants were collected by centrifugation at 17,000 × *g* for 30 min at 4˚C. Protein content was quantified using a Bradford assay (Bio-Rad, Hercules, CA, USA) in an UV spectrophotometer. The cell lysates were separated by 10% SDS polyacrylamide gel electrophoresis (SDS-PAGE). Proteins were transferred to nitrocellulose membranes which were blocked in 5% non-fat dried milk dissolved in Tris buffered saline containing Tween-20 (150 mM NaCl, 20 mM Tris-HCl, pH 7.4, 0.1% Tween-20) for 1 h at room temperature. The membranes were incubated overnight at 4˚C with specific primary antibodies. After washing, the membranes were incubated with the secondary antibodies (HRP conjugated anti-mouse IgG or anti-rabbit) for 1 h at room temperature. After washing, the blots were analyzed using West-Zol Plus and a western blot detection system (iNtRON Biotechnology, Sungnam, Republic of Korea).

Analysis of mitochondrial membrane potential (MMP). Mitochondrial membrane potential (MMP) ($\Delta\psi m$) was determined by $DiOC_6$ staining and measured by flow cytometry. Briefly, A549 cells were cultured in 60 mm culture dishes (2.5×10^5 cells/well) for 24 h, treated with tannic acid and were harvested with trypsin-EDTA. The amount of 0.1 μM of $DiOC_6$ was added and incubated in the dark for 15 min at 37˚C. The cells were centrifuged (300 × *g*, 5 min, 4˚C), and re-suspended in 200 μl of PBS. The solutions were analyzed by FACS Calibur instrument and Cell Quest software (BD Biosciences). The entire protocol was performed in low light.

Mitochondrial isolation. A549 cells were treated with tannic acid and fractionated by using the Mitochondria isolation kit (Thermo Fisher Scientific Inc, Rockford, IL, USA) (BioVision Inc., San Francisco, CA, USA) in accordance with the manufacturer's instructions. The tannic acid-treated and non-treated cells were harvested with trypsin-EDTA and centrifuged at 600 × *g* for 5 min at 4˚C. The cell pellets were suspended in 1 mL cytosol extraction reagent. The suspensions were incubated on ice for 10 min, homogenized in a sonicator, and centrifuged at 16,000 × *g* for 10 min at 4˚C. The supernatant was isolated and centrifuged again at 10,000 × *g* for 30 min at 4˚C; the resulting supernatant, constituting the cytosolic fraction, was transferred to a pre-chilled tube. The resulting pellet, constituting the mitochondrial fraction, was used in subsequent experiments.

Statistical analysis. All data are expressed as mean±standard deviation from three independent experiments. GraphPad Prism software (GraphPad Software, La Jolla, CA, USA) was used to evaluate the data. The statistical significance ($*p<0.05$, $**p<0.01$, or $***p<0.001$) was assessed by student's *t*-test and one-way analysis of variance (ANOVA) followed by *post-hoc* comparison (Tukey's HSD).

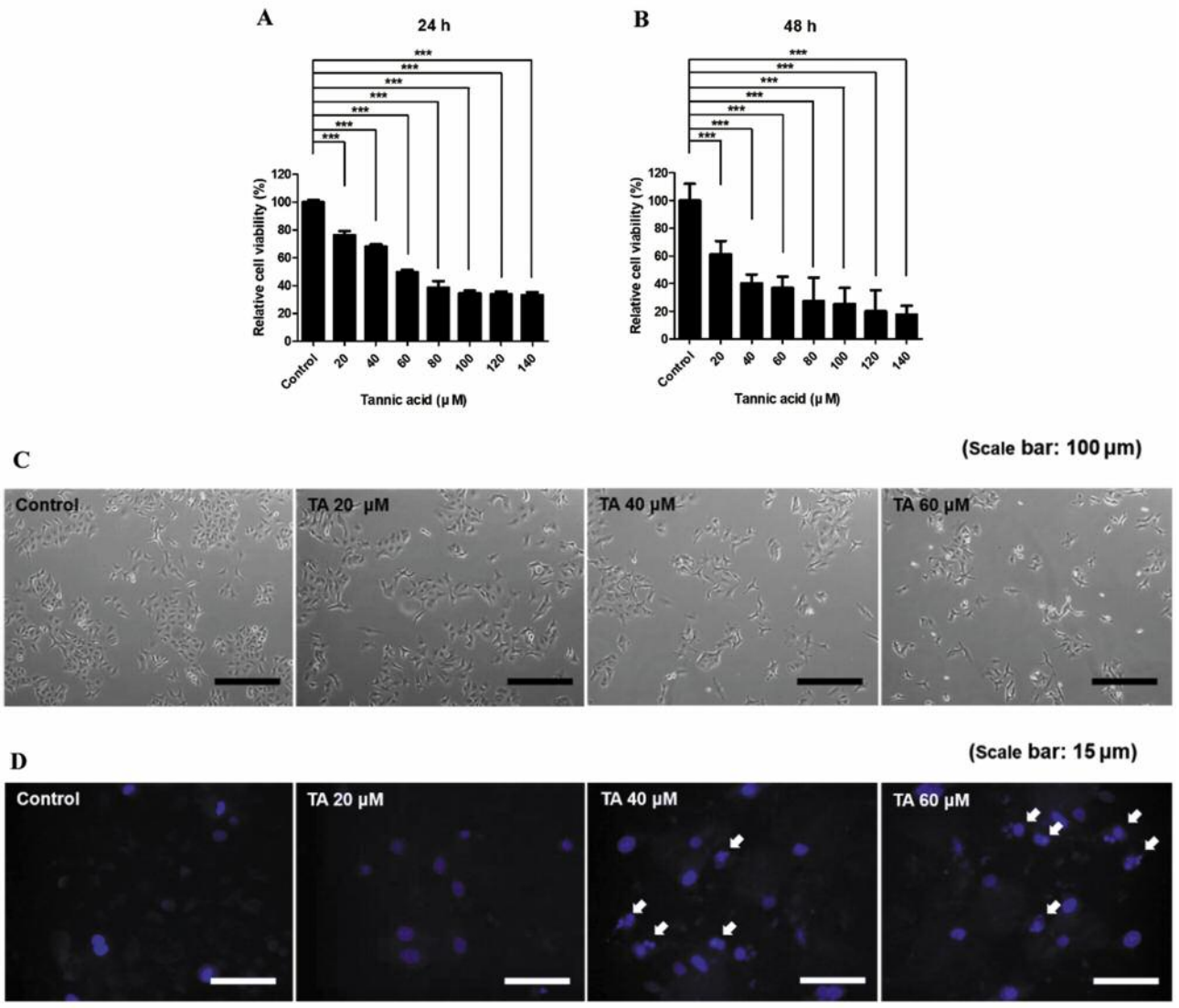

Figure 1. *Effects of tannic acid on the viability and morphology of A549 human lung cancer cells. Cells were treated with various concentrations (0, 20, 40, 60, 80, 100, 120 or 140 μM) of tannic acid for (A) 24 h or (B) 48 h and the cell viability was assessed by the crystal violet assay. Cell viability is presented as percentage relative absorbance in the treated group compared to the control. Data are expressed as the mean±SD of three independent experiments. Asterisk denotes statistical significance (***p<0.001) of post-hoc comparisons (Tukey's HSD) compared to the control. (C) Cells were cultured with 20, 40 or 60 μM of tannic acid for 24 h, observed by phase-contrast microscopy and photographed (ix71, Olympus, japan). Scale bar, 100 μm; (D) Nuclear changes and chromatin condensation were observed in cells treated with 20, 40 or 60 μM tannic acid for 24 h followed by DAPI staining using fluorescence microscopy (ix71, Olympus, japan). Scale bar, 15 μm. TA: Tannic acid.*

Results

Tannic acid suppresses the viability and induces morphological changes and chromatin condensation in A549 cells. The cytotoxicity of tannic acid on A549 lung cancer cells was measured by the crystal violet assay. Cells were treated with various concentrations (0, 20, 40, 60, 80, 100, 120, or 140 μM) of tannic acid for 24 or 48 h. As shown in Figure 1A, tannic acid suppressed cell viability in a dose dependent manner at 24 h; the suppression was higherafter 48 h treatment (Figure 1B). The IC_{50} value of tannic acid was estimated to be between 40 and 60 μM at 24 h and between 20 and 40 μM at 48 h. Based on these results, the morphological changes induced by the compound were examined by treating A549 cells with 20, 40, or 60 μM tannic acid for 24 h. The results showed a decrease in cell confluency as well as an increase in the number of floating and abnormal shaped cells (Figure 1C). In addtion, DAPI staning was

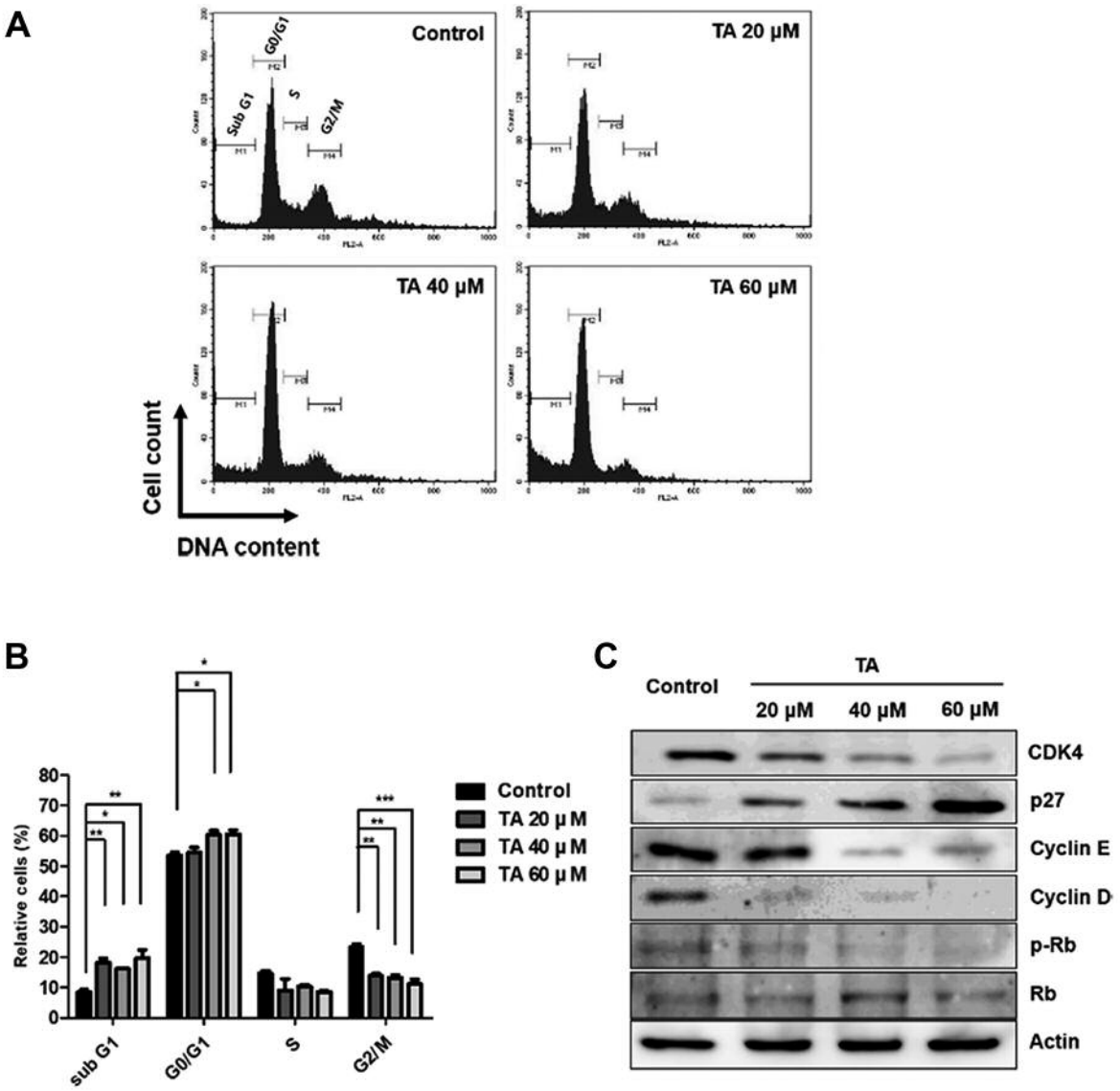

Figure 2. *Effects of tannic acid on cell cycle arrest and the cell cycle regulators in A549 cells. (A) Flow cytometry analysis showing changes in cell cycle after tannic acid treatment and PI staining; (B) Graphical presentation of the relative distribution of cells in the different phases of the cell cycle. Data are expressed as the mean±SD of three independent experiments. Asterisk denotes statistical significance (*p<0.05, **p<0.01, ***p<0.001) of post-hoc comparisons (Tukey's HSD) compared to the control. (C) Expression levels of cyclin dependent kinase 4 (CDK4), P27, cyclin D, cyclin E, retinoblastoma (Rb) and phospho-Rb (p-Rb) in cells treated with tannic acid as assayed by western blot analysis. Actin was used as a housekeeping gene for sample loading. TA: Tannic acid.*

performed to determine chromatin condensation and shrinkage, associated with tannic acid induced apoptosis. The cells were treated with various concentrations of tannic acid (20, 40, or 60 μM) for 24 h, followed by treatment with DAPI for 5 min. As shown in Figure 1D, compared with the control group, the tannic acid-treated group showed a higher number of cells with high fluorescence intensity, indicating an increase in the ratio of cells having condensed and shirinked DNA.

Tannic acid induces G_0/G_1 cell cycle arrest and accumulation of A549 human lung cancer cells in the Sub-G_1 phase of the cell cycle. To evaluate the effect of tannic acid on cell cycle, A549 cells were treated with 20, 40 or 60 μM tannic acid for 24 h and cell cycle arrest was evaluated by PI staining followed by FACS analysis. The results showed that tannic acid induced an accumulation in the sub G_1 phaseand an increase in the G_0/G_1 ratio of A549 cells,

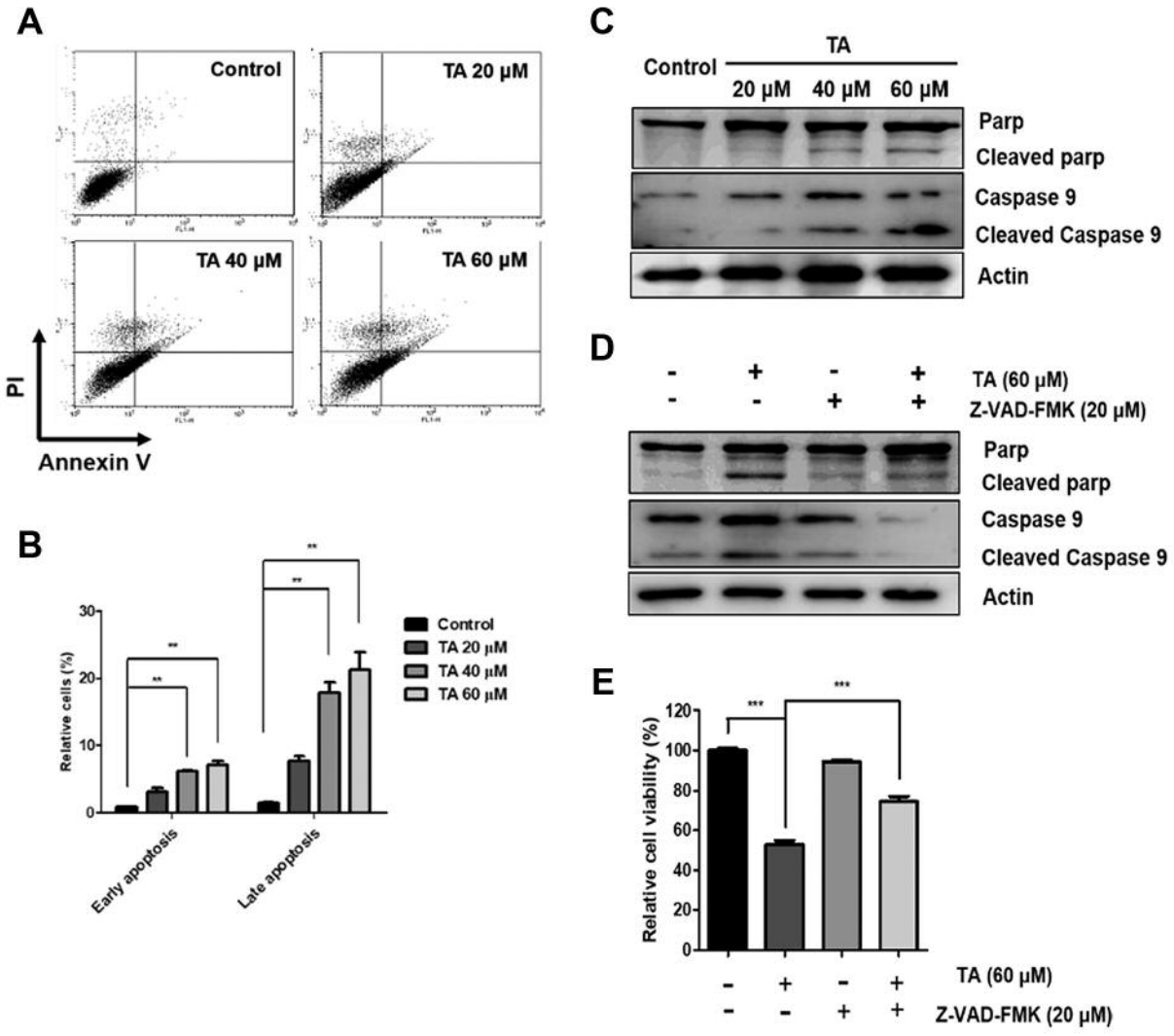

Figure 3. *Tannic acid induces caspase-mediated apoptosis in A549 cells. (A) Annexin V fluorescein isothiocyanate (FITC)/propidium iodide (PI) staining; (B) Graphical presentation indicating relative percentage of apoptotic cells. Data are expressed as the mean±SD of three independent experiments. Asterisk denotes statistical significance (**p<0.01) of post-hoc comparisons (Tukey's HSD) compared to the control; (C) Expression levels of caspase 9, cleaved caspase 9, PARP and cleaved PARP proteins were evaluated using western blotting; (D) Effect of tannic acid and pan caspase inhibitor (Z-VAD-FMK) on the expression levels of cleaved PARP and cleaved caspase 9. Actin was used as an internal control for sample loading; (E) Effect of tannic acid and Z-VAD-FMK on the viability of A549 cells. Data are expressed as the mean±SD of three independent experiments. Asterisk denotes statistical significance (***p<0.001) of post-hoc comparisons (Tukey's HSD) compared to the control. TA: Tannic acid.*

while decreasing the cells in the S phase and the G_2/M ratio of cells (Figure 2A and B). Futhermore, we quantified the expression of cell cycle marker proteins, such as CDK4, p27, cyclin E, cyclin D, Rb and p-Rb using western blotting in A549 cells treated with tannic acid. As shown in Figure 2C, treatment with tannic acid increased expression of p27, whereas, it decreased the expression of cyclin D, cyclin E, CDK4 and p-Rb proteins. These results indicate that tannic acid induces G_0/G_1 cell cycle arrest *via* G_1/S check points. In addition, tannic acid increased the sub-G_1 population of A549 cells, indicating fragmentation of chromatin, which is associated with cell death.

Tannic acid induces cell death via the intrinsic apoptosis pathway. The apoptotic effect of tannic acid was evaluated using the Annexin V FITC/PI staining. Cell surface exposure of phosphatidylserine and increased permeability of nuclear membrane are important characteristics of apoptosis (16). Our data shows that the ratio of annexin V^+/PI^- (early apoptotic cells) and annexin V^+/PI^+ (late apoptotic cells) was

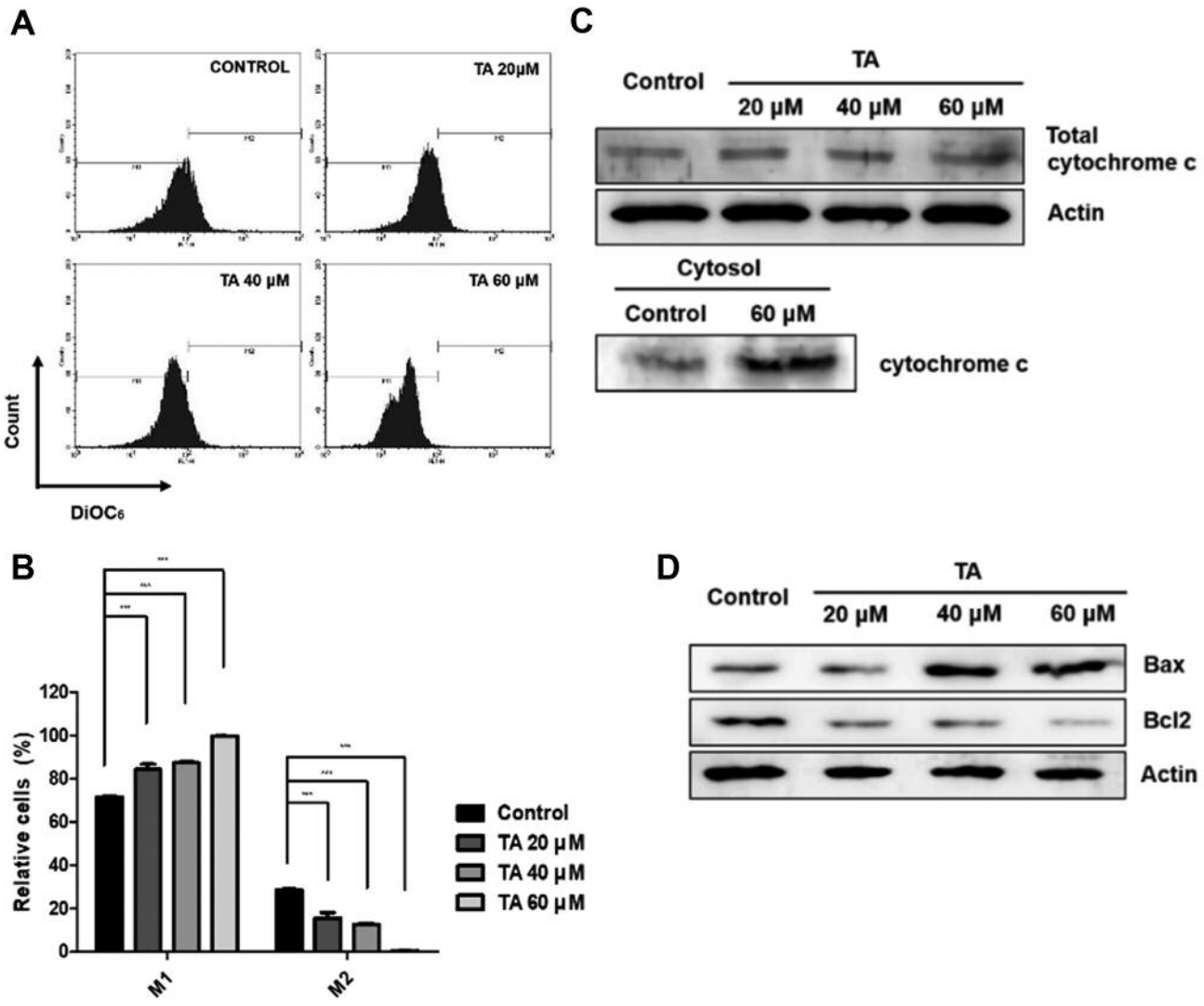

Figure 4. *The mitochondrial pathway is involved in tannic acid induced apoptosis of A549 cells. (A) Change in mitochondrial membrane potential (ΔΨm) of A549 cells by tannic acid treatment, as measured by the $DiOC_6$ staining method; (B) Graphical presentation indicating relative percentage of cells. Data are expressed as the mean±SD of three independent experiments. Asterisk denotes statistical significance (***p<0.001) of post-hoc comparisons (Tukey's HSD) compared to the control; (C) Expression levels of cytochrome c in the cytosolic and mitochondrial fractions; (D) Expression levels of Bax, Bcl2 and Actin. Actin was used as loading control. TA: Tannic acid.*

increased by tannic acid treatment (Figure 3A and B). Subsequently, to explore the detailed mechanisms of tannic acid induced apoptosis, we evaluated the expression levels of PARP and caspase 9 by western blotting (Figure 3C) and found that the expression levels of cleaved caspase 9 and cleaved PARP were increased by tannic acid. Furthermore, treatment of A549 cells with pan caspase inhibitor (Z-VAD-FMK) reduced the expression levels of cleaved caspase 9 and cleaved PARP and rescued the cells from tannic acid induced cytotoxicity (Figure 3D and E). These results indicate that tannic acid induces caspase-mediated programmed cell death in lung cancer cells.

Mitochondria are involved in tannic acid induced apoptosis of A549 cells. Mitochondrial dysfunction is an important aspect of intrinsic apoptosis (17). To evaluate the association of mitochondrial outer membrane pore (MOMP) formation with tannic acid induced cell death, we examined the mitochondrial membrane potential of A549 cells using $DiOC_6$ and determined the expression of cytochrome c in the cytosolic fraction of A549 cells (16). Our results showed that tannic acid treatment resulted in a down-regulation in the relative mitochondrial membrane potential (Figure 4A and B) and up-regulation of the levels of cytosolic cytochrome c (Figure 4B). However, the total amount of cytochrome c was

not changed. In addition, the expression ratio of the Bcl2/Bax genes was disrupted by tannic acid (Figure 4C). These results demonstrate that tannic acid induces disruption of mitochondrial membrane and release of cytochrome c.

Tannic acid suppresses the metastatic potential of A549 cells. The metastatic potential of A549 cells upon tannic acid treatment was evaluated using the wound healing and Matrigel invasion assays. A549 cells show almost complete wound closure after 24 h; however, in cells pre-treated with tannic acid, the wound closer was inhibited in a concentration dependent manner (Figure 5A and B). These results suggested that tannic acid suppresses A549 migration. Matrigel invasion assay is a commonly used method for determining the invasive potential of cancer cells (18). The matrigel invasion assay performed in a pre-coated chamber showed that tannic acid reduced the number of infiltrated cells (Figure 5C). These results indicate that tannic acid inhibits the metastatic potential of A549 cells.

Tannic acid suppresses stemness potential of A549 cells. The effect of tannic acid on the stemness potential of A549 cells was evaluated based on their sphere forming ability. Cells were cultured in an optimized sphere forming media and ultra-low attachment dish for 7 days. Then, the sphere formation was observed after 0, 3 or 7 days of incubation and finally the number of spheres were counted on day 7 using a microscope. In addition, the relative expression of stemness marker genes, SOX2, OCT4 and NANOG were examined. Furthermore, we determined the relative cell population expressing CD133 (one of cell surface stemness markers of A549 cells) in the spheres of A549 cells using FACS analysis. Our results showed a reduction in the number and size of the spheres in the tannic acid treated group (Figure 6A and B). Furthermore, the proportion of cells expressing $CD133^{high}$ was found to be decreased in the tannic acid treated group (Figure 6C and D). The expression levels of stem cell marker genes were found to be decreased by tannic acid treatment (Figure 6E). These results indicate that the stemness potential of A549 cells was suppressed by tannic acid treatment.

Discussion

Although various therapies have been developed for lung cancer, it is still one of the most complex diseases for chemoprevention and treatment (19). Phytochemical-based cancer prevention and treatment provides the possibility to replace or improve the efficiency of existing anticancer drugs by elucidating their effects and mechanisms (8). In particular, polyphenols are the most frequently studied phytochemicals that have useful physiological functions and anticancer effects (20).

Tannic acid is a one of the natural polyphenols that has been recently reported to have anticancer effects on breast (13), colorectal (21), and prostate cancers (22). However, there is no study elucidating the effect of tannic acid on human lung cancer. Therefore, the current study investigated the effects of TA and its underlying mechanisms on the malignant phenotype of A549 lung cancer cells, especially focusing on the proliferation and cell death mechanisms, cell cycle, invasion, migration, and stemness.

The extrinsic and intrinsic apoptotic pathways are cell death mechanisms under investigation and have been identified as important targets for cancer treatment (23). We investigated the mechanisms associated with tannic acid induced cell death. Tannic acid has been already known to induce mitochondrial apoptotic pathways in breast and gingival cancer, however, the detailed mechanisms have not been elucidated (13, 14). In the current study, tannic acid treatment results in abnormal shaped and floating A549 cancer cells (Figure 1A). Further, chromatin condensation and nuclear outer membrane pore formation were induced by tannic acid treatment (Figure 1B). In addition, an elevation in the ratio of annexin V^+/PI^+ cells was observed (Figure 3B). These changes are commonly observed during apoptosis, which indicate the flip flop of phosphatidylserine and changes in nuclear permeability (24). Further, tannic acid increases the levels of cleaved caspase 9 and cleaved PARP (Figure 3C). However, cell viability associated changes were partially recovered following treatment with the pan caspase inhibitor treatment (Figure 3A, D and E). These results indicate that the caspase cascade is induced by tannic acid and has an important role in A549 induced cell death. Furthermore, our results indicate the involvement of mitochondria in tannic-acid-induced apoptosis of A549 cells. We observed an inhibition in mitochondrial membrane potential and BCL2 gene expression in tannic-acid-induced apoptosis (Figure 4A, B and D). In addition, the cytosolic levels of cytochrome c were found to be increased by tannic acid (Figure 4C). At the same time, the extrinsic apoptosis associated marker was not detected. These results indicate that tannic acid induces cell death of A549 cells through the mitochondrial apoptotic (intrinsic) pathway.

Another important effect of tannic acid on A549 cells is induction of cell cycle arrest. In previous studies related to breast and gingival cancer, tannic acid induced G_0/G_1 cell cycle arrest (13, 14). In breast cancer cells, tannic acid was thought to bind directly to the growth factor receptors, such as EGFR and IGFR, thereby suppressing cell proliferation, however, the detailed mechanisms were not studied. Our cell cycle analysis data showed that tannic acid induces cell cycle arrest in the G_0/G_1 phase in A549 cells (Figure 2A and B). Furthermore, we found that the expression levels of cyclin D and cyclin E were reduced, while the expression levels of p27 were increased (Figure 2C). Consequently, phosphorylation of retinoblastoma protein (Rb) was inhibited (Figure 2C).

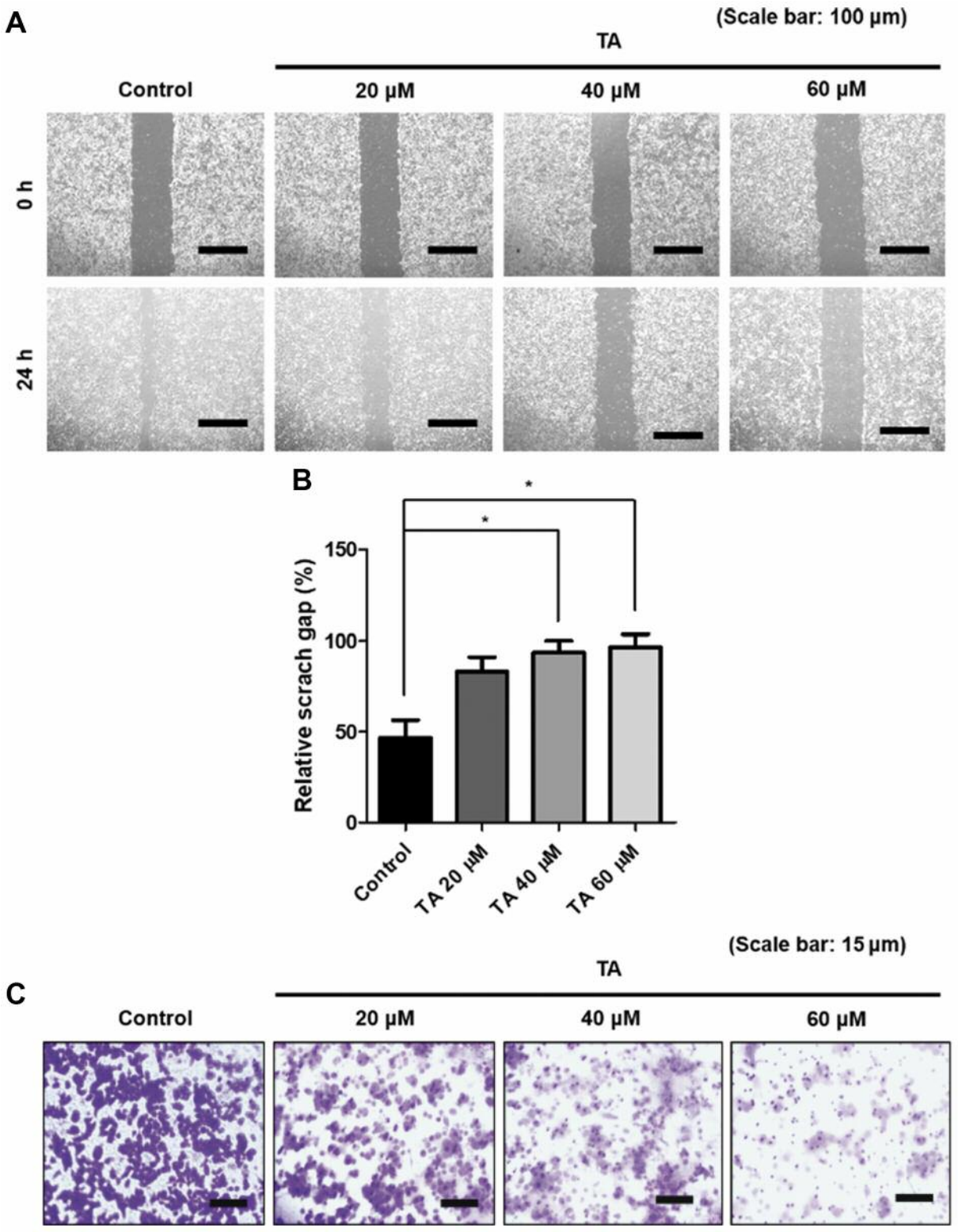

Figure 5. *Tannic acid inhibits migration and invasion potential of A549 cells. (A) Changes in wound closure ability of cells after tannic acid treatment, which were quantified using image J software. Representative photographs are presented (scale bar, 100 μm); (B) Graphical presentation indicating relative percentage scratch gap. Data are expressed as the mean±SD of three independent experiments. Asterisk denotes statistical significance (*p<0.05) of post-hoc comparisons (Tukey's HSD) compared to the control; (C) Effect of tannic acid on the invading ability of lung cancer cells through matrigel. Representative photographs indicating the invading cells are presented (scale bar, 15 μm). TA: Tannic acid.*

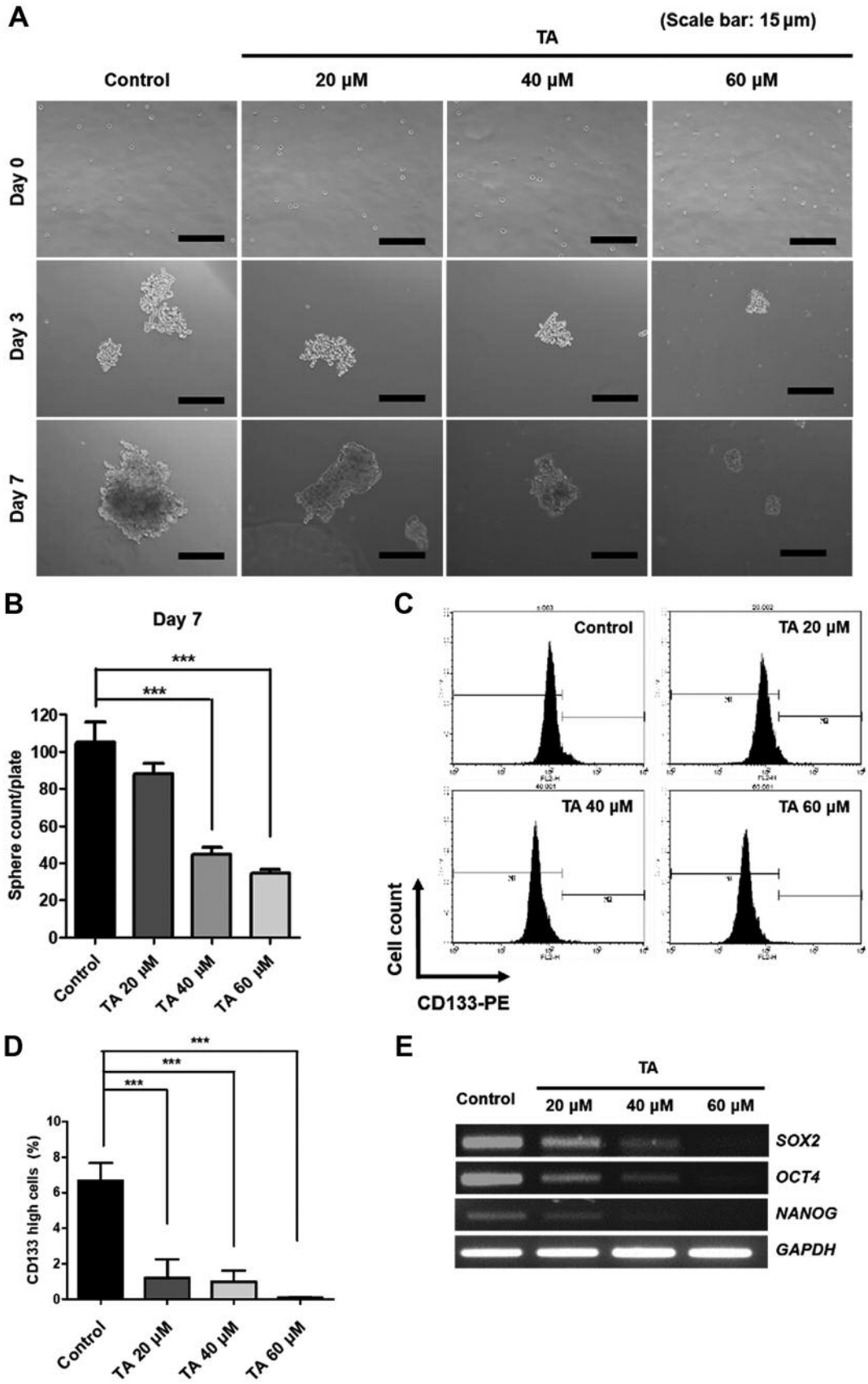
A
(Scale bar: 15 μm)
TA
Control
20 μM
40 μM
60 μM
Day 0
Day 3
Day 7
B
Day 7
***
***
Sphere count/plate
120
100
80
60
40
20
0
Control
TA 20 μM
TA 40 μM
TA 60 μM
C
Control
TA 20 μM
TA 40 μM
TA 60 μM
Cell count
CD133-PE
D
***
***
***
CD133 high cells (%)
10
8
6
4
2
0
Control
TA 20 μM
TA 40 μM
TA 60 μM
E
TA
Control
20 μM
40 μM
60 μM
SOX2
OCT4
NANOG
GAPDH

These results indicate a possible mechanism associated with cell cycle arrest of lung cancer cells.

Furthermore, tannic acid inhibited the invasion and migration ability of A549 cells, which are important for epithelial mesenchymal transition of metastatic lung cancer cells and are associated with the stemness potential of cancer cells (25, 26).We observed that tannic acid decreased wound healing ability and cell invasion through matrigel (Figure 5A and B). Similar results have been observed in a previous study in prostate cancer cells (27). We hypothesized that these characteristics might be related to the stemness of A549 cells, which led us to investigate the stemness potential of A549 cells by the sphere forming assay and determine the expression of stemness markers. We found that the size and number of spheres were reduced by tannic acid treatment (Figure 6A and B). Furthermore, the expression levels of SOX2, OCT4 and NANOG, markers of cancer stem cells (28), as well as the percentage of cells over-expressing CD133 were found to be decreased (Figure 6C, D and E).

In this study, we provide evidence that tannic acid can suppress growth of A549 lung cancer cells by triggering caspase-dependent mitochondrial-mediated apoptosis, as well as cell cycle arrest. Furthermore, this study shows that tannic acid reduces the metastatic and stemness potential of A549 cells.

Conflicts of Interest

The Authors declare no conflicts of interest regarding this study.

Authors' Contributions

Y.M.Y. and K-J.J. designed the experiments. N.S., D.Y.K., and D.H.K. conducted the most of experiments. J-S.Y., E.S.J., and A.R. helped in some experiments. Y.M.Y., K-J.J., D.H.K., N.S., and D.Y.K. evaluated the data, and K-J.J. wrote the manuscript. All Authors contributed in revising the manuscript and agreed for the final version for submission.

←

Figure 6. *Tannic acid suppresses stemness potential of A549 cells. (A) Change in sphere forming ability of A549 cells by tannic acid treatment. Representative photographs are presented (scale bar, 15 μm). Cells were incubated with sphere forming media for 7 days with different concentrations of tannic acid; (B) Effects of tannic acid on the number of spheres of A549 cells after 7 days of incubation; (C) Relative expression of CD133 cell surface marker; (D) Graphical presentation indicating the relative ratio of CD133high population of A549 cells. Data are expressed as the mean±SD of three independent experiments. Asterisk denotes statistical significance (***p<0.001) of post-hoc comparisons (Tukey's HSD) compared to the control; (E) mRNA expression levels of SOX2, OCT4, NANOG, and GAPDH genes. GAPDH was used as housekeeping gene for sample loading. TA: Tannic acid.*

Acknowledgements

This work was supported by the National Research Foundation of Korea (NRF) grant funded by the Korean government (MSIT) (No. 2018R1C1B6006146) and by Basic Science Research Program through the National Research Foundation of Korea (NRF) funded by the Ministry of Education (No. 2018R1D1A1B07048651, 2019R1I1A1A01060399, and 2019R1I1A1A01060537).

References

1 Inamura K: Lung cancer: Understanding its molecular pathology and the 2015 who classification. Front Oncol *7*: 193, 2017. PMID: 28894699. DOI: 10.3389/fonc.2017.00193

2 Griesinger F: Current aspects of diagnosis and treatment of lung cancer. Dtsch Med Wochenschr *142(24)*: 1808-1812, 2017. PMID: 29207424. DOI: 10.1055/s-0043-112779

3 Patel N, Adatia R, Mellemgaard A, Jack R and Møller H: Variation in the use of chemotherapy in lung cancer. Br J Cancer *96(6)*: 886-890, 2007. PMID: 17342091. DOI: 10.1038/sj.bjc.6603659

4 Oun R, Moussa YE and Wheate NJ: The side effects of platinum-based chemotherapy drugs: A review for chemists. Dalton Trans *47(19)*: 6645-6653, 2018. PMID: 29808879. DOI: 10.1039/c8dt00838h

5 Uramoto H and Tanaka F: Recurrence after surgery in patients with nsclc. Transl Lung Cancer Res *3(4)*: 242-249, 2014. PMID: 25806307. DOI: 10.3978/j.issn.2218-6751.2013.12.05

6 Priyadarsini RV and Nagini S: Cancer chemoprevention by dietary phytochemicals: Promises and pitfalls. Curr Pharm Biotechnol *13(1)*: 125-136, 2012. PMID: 21466433. DOI: 10.2174/138920112798868610

7 Surh YJ: Cancer chemoprevention with dietary phytochemicals. Nat Rev Cancer *3(10)*: 768-780, 2003. PMID: 14570043. DOI: 10.1038/nrc1189

8 Kang DY, Sp N, Jo ES, Rugamba A, Hong DY, Lee HG, Yoo JS, Liu Q, Jang KJ and Yang YM: The inhibitory mechanisms of tumor pd-l1 expression by natural bioactive gallic acid in non-small-cell lung cancer (nsclc) cells. Cancers (Basel) *12(3)*, 2020. PMID: 32204508. DOI: 10.3390/cancers12030727

9 Byun HJ, Darvin P, Kang DY, Sp N, Joung YH, Park JH, Kim SJ and Yang YM: Silibinin downregulates mmp2 expression *via* jak2/stat3 pathway and inhibits the migration and invasive potential in mda-mb-231 cells. Oncol Rep *37(6)*: 3270-3278, 2017. PMID: 28440514. DOI: 10.3892/or.2017.5588

10 Sp N, Kang DY, Joung YH, Park JH, Kim WS, Lee HK, Song KD, Park YM and Yang YM: Nobiletin inhibits angiogenesis by regulating src/fak/stat3-mediated signaling through pxn in er(+) breast cancer cells. Int J Mol Sci *18(5)*, 2017. PMID: 28468300. DOI: 10.3390/ijms18050935

11 Sp N, Kang DY, Kim DH, Park JH, Lee HG, Kim HJ, Darvin P, Park YM and Yang YM: Nobiletin inhibits cd36-dependent tumor angiogenesis, migration, invasion, and sphere formation through the cd36/stat3/nf-kappab signaling axis. Nutrients *10(6)*, 2018. PMID: 29914089. DOI: 10.3390/nu10060772

12 Booth BW, Inskeep BD, Shah H, Park JP, Hay EJ and Burg KJ: Tannic acid preferentially targets estrogen receptor-positive breast cancer. Int J Breast Cancer *2013:* 369609, 2013. PMID: 24369505. DOI: 10.1155/2013/369609

13 Darvin P, Joung YH, Kang DY, Sp N, Byun HJ, Hwang TS, Sasidharakurup H, Lee CH, Cho KH, Park KD, Lee HK and Yang

YM: Tannic acid inhibits egfr/stat1/3 and enhances p38/stat1 signalling axis in breast cancer cells. J Cell Mol Med *21(4)*: 720-734, 2017. PMID: 27862996. DOI: 10.1111/jcmm.13015

14 Darvin P, Baeg SJ, Joung YH, Sp N, Kang DY, Byun HJ, Park JU and Yang YM: Tannic acid inhibits the jak2/stat3 pathway and induces g1/s arrest and mitochondrial apoptosis in yd-38 gingival cancer cells. Int J Oncol *47(3)*: 1111-1120, 2015. PMID: 26202061. DOI: 10.3892/ijo.2015.3098

15 Sp N, Kang DY, Jo ES, Rugamba A, Kim WS, Park YM, Hwang DY, Yoo JS, Liu Q, Jang KJ and Yang YM: Tannic acid promotes trail-induced extrinsic apoptosis by regulating mitochondrial ROS in human embryonic carcinoma cells. Cells *9(2)*, 2020. PMID: 31979292. DOI: 10.3390/cells9020282

16 Reed JC: Mechanisms of apoptosis. Am J Pathol *157(5)*: 1415-1430, 2000. PMID: 11073801. DOI: 10.1016/S0002-9440(10)64779-7

17 Wang C and Youle RJ: The role of mitochondria in apoptosis. Ann Rev Genet *43:* 95-118, 2009. PMID: 19659442. DOI: 10.1146/annurev-genet-102108-134850

18 Shaw LM: Tumor cell invasion assays. *In*: Cell migration: Developmental methods and protocols. Guan J-L (ed.). Humana Press: Totowa, NJ, pp. 97-105, 2005. PMID: 15576908. DOI: 10.1385/1-59259-860-9:097

19 Torre LA, Siegel RL and Jemal A: Lung cancer statistics. Adv Exp Med Biol *893:* 1-19, 2016. PMID: 26667336, DOI: 10.1007/978-3-319-24223-1_1

20 Zhou Y, Zheng J, Li Y, Xu DP, Li S, Chen YM and Li HB: Natural polyphenols for prevention and treatment of cancer. Nutrients *8(8)*, 2016. PMID: 27556486, DOI: 10.3390/nu8080515

21 Cosan D, Soyocak A, Basaran A, Degirmenci I and Gunes H: The effects of resveratrol and tannic acid on apoptosis in colon adenocarcinoma cell line. Saudi Med J *30:* 191-195, 2009. PMID: 19198704.

22 Karakurt S and Adalı O: Tannic acid inhibits proliferation, migration, invasion of prostate cancer and modulates drug metabolizing and antioxidant enzymes. Anticancer Agents Med Chem *16*, 2015. PMID: 26555610. DOI: 10.2174/1871520616666151111115809

23 Ichim G and Tait SWG: A fate worse than death: Apoptosis as an oncogenic process. Nat Rev Cancer *16(8)*: 539-548, 2016. PMID: 27364482. DOI: 10.1038/nrc.2016.58

24 Rieger AM, Nelson KL, Konowalchuk JD and Barreda DR: Modified annexin v/propidium iodide apoptosis assay for accurate assessment of cell death. J Vis Exp *50*: 2597, 2011. PMID: 21540825. DOI: 10.3791/2597

25 Brabletz T, Kalluri R, Nieto MA and Weinberg RA: Emt in cancer. Nat Rev Cancer *18(2)*: 128-134, 2018. PMID: 29326430. DOI: 10.1038/nrc.2017.118

26 Singh A and Settleman J: Emt, cancer stem cells and drug resistance: An emerging axis of evil in the war on cancer. Oncogene *29(34)*: 4741-4751, 2010. PMID: 20531305. DOI: 10.1038/onc.2010.215

27 Serdar K and Orhan A: Tannic acid inhibits proliferation, migration, invasion of prostate cancer and modulates drug metabolizing and antioxidant enzymes. Anticancer Agents Med Chem *16(6)*: 781-789, 2016. PMID: 26555610. DOI: 10.2174/1871520616666151111115809

28 Chen K, Huang YH and Chen JL: Understanding and targeting cancer stem cells: Therapeutic implications and challenges. Acta Pharmacol Sin *34(6)*: 732-740, 2013. PMID: 23685952. DOI: 10.1038/aps.2013.27

Received April 23, 2020
Revised May 7, 2020
Accepted May 12, 2020